

Research Paper

## Deformation Events and Structural History of the High Grade Granulite Terrain around Polur, Thiruvannamalai District Tamilnadu, South India

A.V. George\*, K. Shankar

Adama Science and Technology University, School of Applied Natural Sciences, Department of Applied Geology, Adama, Ethiopia

\* Corresponding author, e-mail: [aikaravgeorge@gmail.com](mailto:aikaravgeorge@gmail.com)

### Abstract

The objective of the present study is to establish the structural history and deformation episodes present in the area. The techniques used are Preparation of structural map of the area from primary data and subsequent structural analysis by preparing Pie diagrams. The Study reveals that the complex structural pattern observed is the result of overprinting and interference of structures generated during two different deformation episodes. Folds of different generations represented by  $F_0$ ,  $F_1$ ,  $F_2$ ,  $F_3$  and  $F_4$ , are present throughout the area. At places  $F_1$  folds are intrafolial and rootless. Due to the tightness of  $F_1$  fold  $S_0$  and  $S_1$  are effectively parallel, except in  $F_1$  fold closures where  $S_1$  cuts across  $S_0$ . Map scale  $F_2$  folds identified as Kommandal antiform and Padagam synform, are characterized by thickening of the hinges and thinning of the limbs indicating that the rocks were sufficiently ductile to allow flowage during deformation.  $F_3$  folds with an E-W to NW-SE axial trend have constant orthogonal thickness. Interference of  $F_3$  with  $F_1$  and  $F_2$  has resulted in plunging and eyed folds.  $F_4$  folds are expressed as extremely broad open flexures, with a constant NW-SE trend and postdates major folds. However, faults trending E-W affect  $F_3$  folds and pre date  $F_4$ . The various structures found in the area were formed during deformational events-DI and DII. The evolutionary history of the area worked out on the basis of structural analysis can serve as a model for similar areas of high-grade granulite terrains in other parts of the world.

**Keywords:** - Deformation events, Structural history, granulite terrain, planar structures.

### 1. Introduction

High-Grade Granulite Terrain of South India around Polur, covering an area of 700 sq. km and falling within N latitude  $12^{\circ}15'$ ,  $12^{\circ}35'$  and E longitude  $70^{\circ}3'$  and  $70^{\circ}15'$  are presented. The major litho units are charnockite, Banded Magnetite Quartzite, Pyroxene granulite and granite.

Like most of the other shield areas of the world, in South Indian shield too, vast expanses of high grade rocks occur in close proximity with low grade granite-greenstone belts forming the Granulite Mobiles Belt of South India. As in many other shield areas, in South India too, the high grade granulite terrain received more attention than the neighboring mobile belt. Many geologist such as Holland (1900), Krishnan (1958), Sugavanam et al. (1976), Raith et al. (1983), Hansen et

al. (1985 a,b), Grew and Manton (1986), and Jackson et al. (1988) took active interest in the studies on varies aspects pertaining to high grade granulite terrain like pressure – temperature regime; tectonic aspect, geochemistry of rocks, etc. The last couple of decades have witnessed renewed interest in the study of Precambrian terrains, especially where inferred lower crustal rocks, characterized by granulite grade metamorphism are exposed (Park and Tarnag, 1987; Gullay, 1985; Kroner et al., 1988; Joy Gopal et al., 2004; Talari Rama Krishnah Chetty and Bhaskara Rao, 2006; Goodness et al., 2013; Ligangzhoa et al., 2017).

Based on studies in South African shield, Anhaeusser et al. (1969) introduced the concept of mobile belt. In India the term Charnockite Mobile Belt

(CMB) was introduced by Swaminath et al. (1974). The rocks within the belt are highly deformed with linear, tight, isoclinal fold zones. Lineaments and faults seem to control the distribution of many of the rocks of the mobile belt. The CMB is considered as thrust over the craton by collision tectonics. According to Mahadwan, (1976), the granulite facies metamorphic belt is a plate evolved in the deep, dry zones of the early Precambrian crust. Its geological identity has been partially destroyed by the late Precambrian metamorphic and tectonic events. Thus the granulite mobile belt of India is considered as a true mobile belt of Archean age, reworked by Proterozoic deformation and metamorphism, which represents deep seated segments, reactivated and brought to the surface through repeated uplifts.

## 2. Methodology and Field Setting

### 2.1. Methodology

The methodology followed in the present investigation is preparation of base map from toposheets and collection of primary data during field trips. Structural analysis were carried out by preparing lithological (Figure 1) and structural maps (Figure 2).

### 2.2. Field setting

The study area forms part of the Thiruvannamalai district of Tamilnadu. Foliated Charnockite (Charnockite gneiss) constitute the predominant rock unit. Conformable bands and lenses of pyroxene granulite are observed with in the Charnockite gneiss. The meta sedimentary variants of the Precambrian metamorphics are represented by Banded Magnetite Quartzite (BMQ). It is observed as bands with considerable strike persistence inter layered and co folded with Charnockite and pyroxene granulite. Non foliated pink granite is seen as concordant bodies. It is mostly localized at the hinges and is also seen as impersistent bodies in the limbs of folds (Figure 1, 2). Both concordant and discordant veins of quartz and pegmatite are noticed in Charnockite, pyroxene granulite and BMQ. The pegmatite veins vary in thickness from few centimeters up to 50 cm. Local development of tension gashes in pyroxene granulite and Charnockite suggests local shearing (Figure 3). Minor faults and shears are common in BMQ (Figure 4).

Quartz veins, 10-20 cm thick and showing discordant relationship with primary quartz magnetic layers are also noticed (Figure 5). These quartz veins may have resulted from fluids generated within the iron formations during metamorphism, as in the case of iron ore in Minaz Gercis and Middle back Ranges, Australia (Dorr, 1965) and parts of Krivoy Rog in USSR (in Cannon, 1976). Local development of migmatites, considerably altering megascopic characters of pyroxene granulite and Charnockite, is seen towards south of Sananandal (Figure 6). Unmetamorphosed dolomite dykes constitute the younger rock unit. BMQ, showing primary sedimentary layering, with alternate quartz and magnetite layers has considerable strike persistence and positive topographic expression. Hence BMQ bands are ideal marker horizon. The pyroxene granulite bands in many cases have good strike persistence and are of limited use as markers.

## 3. Results and Discussion

### 3.1. Structure

Structural analysis helps to arrive at datum lines which are useful in establishing the chronology of deformational and metamorphic events. The planar structures present are designated in chronological order as  $S_0, S_1, S_2$ , etc. and the linear structures as  $L_1, L_2, L_3$ , etc. Folds combine both planner and linear elements and therefore treated separately. Contacts between lithological units, bedding surfaces and layering in BMQ constitute the earliest planner surface. Pinching and swelling of layers of iron oxide have given rise to lenses and pods (Figure 7). According to Beukes (1973), these are produced by differential compaction and dehydration of parental gelatinous material and the structures are characteristic of the magnetite sub-facies of iron formation. Ptygmatically folded quartz veins, similar to the ones seen in the present area (Figure 8) have been reported by Mason (1970) and in Beukes (1973) from the banded iron formation of the Tati greenstone belts. Boudins of quartz rotated due to deformation is also noticed (Figure 9). These could be of tectonic origin also. Occasional relict intra formational or penecontemporaneous  $F_0$  folds (Figure 10) have also been noticed. These are the earliest folds.

### 3.2. Foliation and cleavages

Metamorphic foliation ( $S_1$ ) is the most widely developed penetrative secondary planar structure and is defined by the preferred orientation of mineral flakes and grains. In pyroxene granulite,  $S_1$  results from preferred orientation of pyroxene prisms and flakes of biotite. Dimensional orientation of magnetite crystals and elongate grains of quartz are responsible for

foliation in BMQ. Foliation, which is sub parallel to  $S_0$ , trends generally in a NNE-SSW to NS and is characterized by high angle of dip. However, due to superposed folding, at places foliation attitude shows variations. Sporadic development of fracture cleavage ( $S_2$ ) at high angles to  $S_0$  and  $S_1$ , is observed mostly in magnetite quartzite (Figure 11). Shear fractures, along which displacements has taken place, have also been observed (Figure 12).

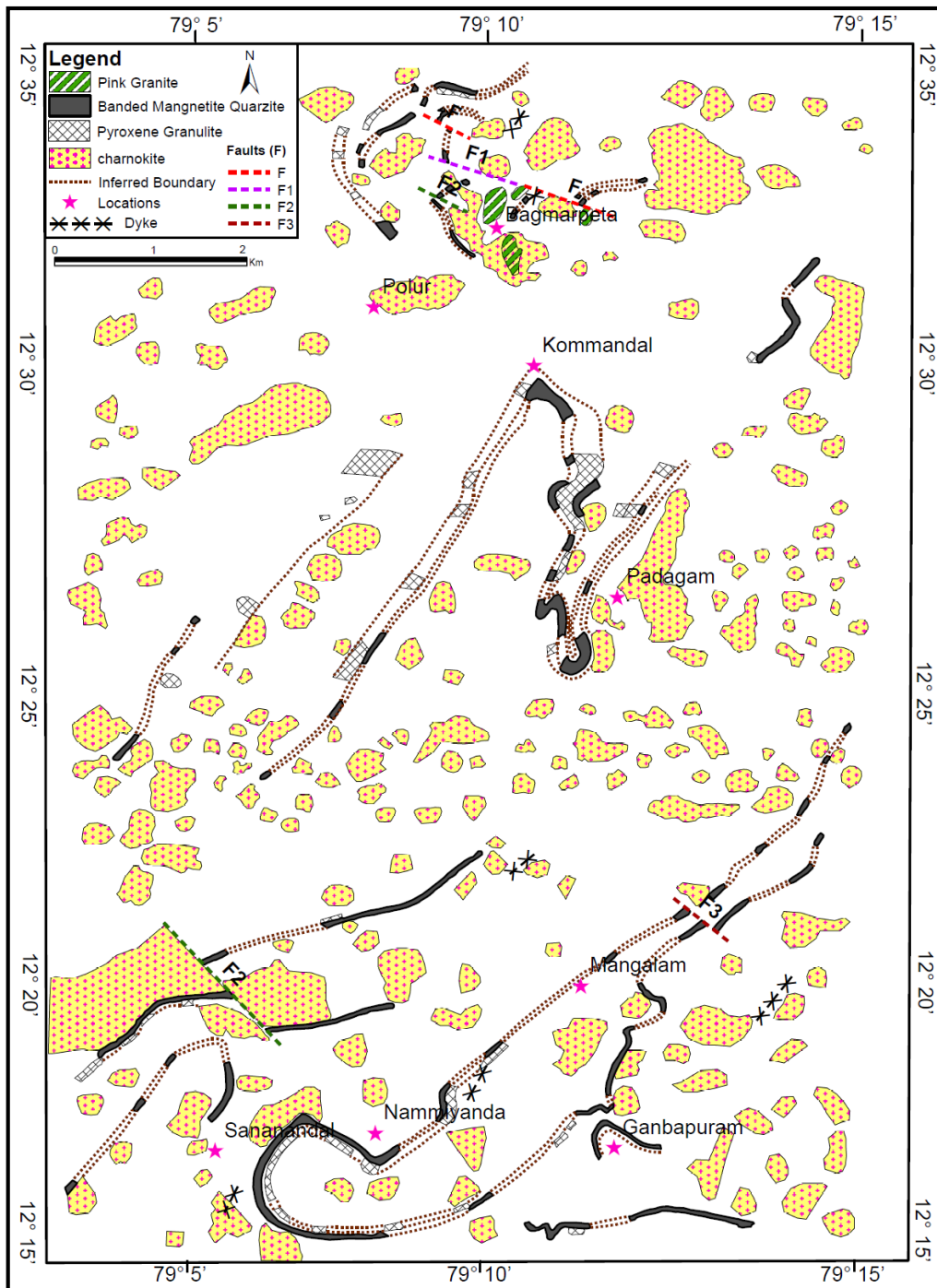


Figure 1: Lithological map of the area around Polur

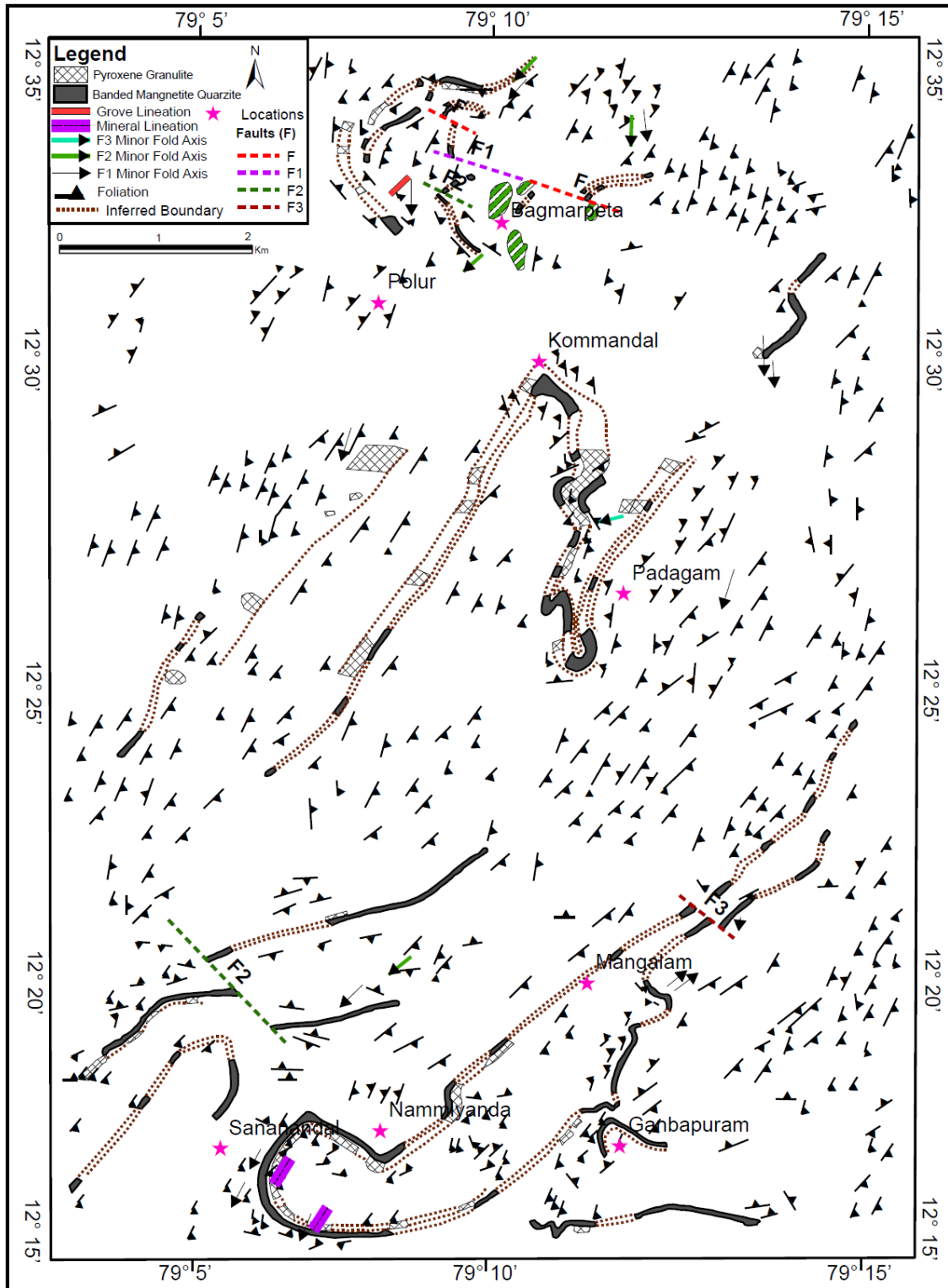


Figure 2: Structural map of the area around Polur

### 3.3. Mineral and groove lineation

In pink granite, mineral lineation  $L_1$  is defined by elongate grains of quartz.  $L_1$  formed by magnetite needles

plunges towards NNE or SSW.  $L_1$  is also parallel or sub parallel to the axes of the earliest folds ( $F_1$ ). Groove lineation.  $L_2$ , observed in pyroxene granulite and BMQ plunges moderately towards SW or NE.



Figure 3: Tension gashes in pyroxene granulite

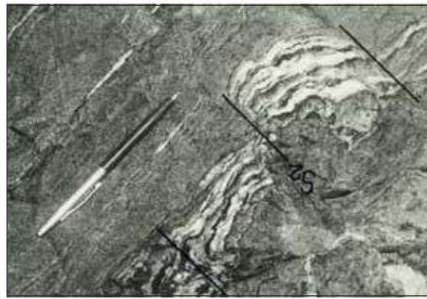


Figure 4: Shear  $S_2$  fracture in BMQ

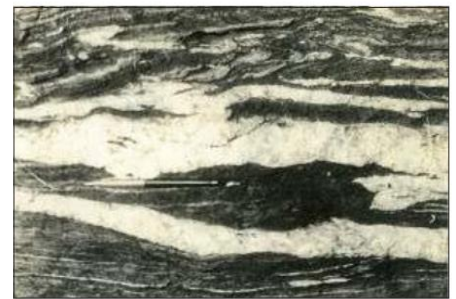


Figure 5: Quartz vein showing discordant relationship with primary quartz magnetite in BMQ



Figure 6: Development of migmatite structure in pyroxene granulite



Figure 7: Pinch and swell structure in magnetite layers in BMQ



Figure 8: Ptygmatically folded quartz in BMQ



Figure 9: Boudin of quartz, rotated due to deformation

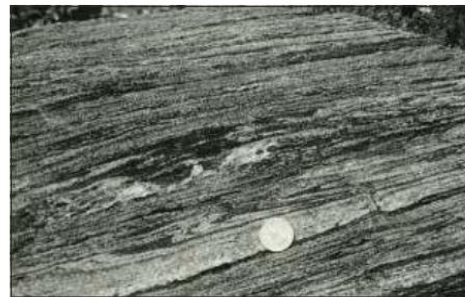


Figure 10: Intraformational  $F_0$  fold in BMQ

### 3.4. Folds

Detailed study of structures, on both mesoscopic and macroscopic scales, reveals that the rocks of the area bear the imprints of four phases of folding –  $F_1$ ,  $F_2$ ,  $F_3$  and  $F_4$ . Folds of each phase have characteristic geometry and orientation (Figure 13). Distinction of folds is based on shape, style, orientation of hinge line and effects of superposed folding, chronology of formation of planar and linear structures and interference pattern (Figure 14, 15).

**3.4.1.  $F_1$  Folds:** Represented by both minor and major folds, are present throughout the study area. These asymmetric, nearly isoclinal, tightly appressed folds have drawn out limbs and thickened hinges (Figure 16).

Due to tightness, the limbs may coalesce leading to repetition and consequent exaggerated thickness of layers (Figure.17).  $F_1$  minor folds are distinguished from penecontemporaneous folds ( $F_0$ ) by the presence of axial planar foliation ( $S_1$ ) associated with  $F_1$ . At places  $F_1$  folds are intrafolial (Figure.18) and root less (Figure. 19), on account of the formation of drawn-out limbs and transposition of foliation on layering. Amplitude of these folds are many times the wavelength, inter limb angle being around  $30^\circ$ . They affect the lithologic layering  $S_0$ . Thickening of the noses is a common feature. The dominant axial trend of  $F_1$  folds is either N-S or NNE-SSW. Due to superposed folding deformation of the axial planes and steeping of the fold axes are also

observed.  $F_1$  fold plunge either towards NNE or SW. Formation of  $F_1$  folds and development of penetration foliations  $S_1$ , are synchronous. In BMQ, in  $F_1$  fold closures, needless of magnetite defining  $S_1$ , cut across layering ( $S_0$ ). On a mesoscopic scale the axial planar nature of  $S_1$  is clear in the closure of the map scale Sananandal  $F_1$  fold (Figure 2), the axial trace of which trends N-S. Due to the tightness of  $F_1$  folds,  $S_0$  and  $S_1$  are effectively parallel in the area except in  $F$  fold closures where  $S_1$  cuts across  $S_0$ .

3.4.2.  $F_2$  folds:  $F_2$  folds too are represented by both major and minor ones (Figure 20). These are folds developed on both  $S_0$  and  $S_1$ .  $F_2$  folds are co-axial with  $F_1$  (Figure 21). The axial planes of  $F_1$  folds have been deformed during  $F_2$  folding. Refolding of  $F_1$  by  $F_2$  has produced 'hook shaped' interference pattern. Though the axes of  $F_1$  and  $F_2$  folds are nearly parallel, i.e. NNE to NE, their geometry is different.  $F_2$  folds are more open, asymmetrical to symmetrical and have higher wavelength /amplitude ratio than  $F$  folds. The inter limb angle' ( $30^\circ$ - $70^\circ$ ) is also larger. In some cases superposed folding has led to tightening of  $F_2$  folds, there by imparting a geometry similar to that of  $F_1$  folds. The axial traces trend NNE-SSW to NE-SW.  $F_2$  folds show variation in plunge possibly, due to superposed folding.  $F_2$  folds on map-scale are observed at three places-near Kommandal, Padagam and Nammiyandal villages.

The northerly trending strike ridge extending from Kommandal to Padagam Village takes a sharp turn near Padagam forming the closure of a map-scale  $F_2$  fold. This fold plunging  $30^\circ$  towards  $N40^\circ$  and closing towards south is a synform, named after Padagam Village, located close to the closure. The two limbs of the fold, marked by BMQ, are so close to each other due to extreme tightness of the fold that these might be taken as a single unit. However, there is a thin pyroxene granulite band separating the two. Foliation ( $S_1$ ) is parallel to the NNE-SSW trending axial plane on the limbs of the synform. But in the closure foliation is folded. The Padagam synform, in addition to being tighter than the Kommandal antiform, is also refolded by another mesoscopic  $F_2$  fold, affecting its western limb. Refolding has resulted in variable foliation attitude in the western part of the closure (Figure 2), the later NE-SW trending  $F_2$  fold being nearly isoclinal.

The Kommandal antiform, named after Kommandal Village is situated very near to its closure. The SSE-trending strike ridge, forming the western, limb of the Padagam synform, turns SSW and defines a tight closure near Kommandal Village. This fold, closing towards north, is considered as an antiform. The closure and the eastern limb of these fold is expressed physiographically north, is considered an antiform. Near the closure of the fold, the ridge after attaining an attitude of 213 m, swings sharply towards SSW (Fig. 23). The Kommandal antiform and the Padagam synform are also characterized by thickening of the closure and thinning of the limbs, indicating that the rocks were sufficiently ductile to allow flowage during deformation.

The third major  $F$  fold is represented by an antiform plunging  $35^\circ$  towards SSW. This fold trending NNE-SSW closes towards south near the village Nammiyandal. It is an antiform because the 'V' of the outcrop points towards the direction of plunge. This  $F_2$  fold has refolded the  $F_1$  synform resulting in 'hook shaped' interference pattern.

3.4.3.  $F_3$  Folds: Broad, open, shallow plunging  $F_3$  cross folds exhibit very low amplitude / wave length ratio, the inter limb angle being  $>130^\circ$  (Figure 2). The plunge direction varies from E to SE and W to NW. They can be easily distinguished from  $F_1$  and  $F_2$  by E-W to NW-SE trending axial trace and large wavelength. All the pre- $F_3$  planar and linear fabrics are affected by  $F_3$  folds. A quartz vein, developed sub parallel to the early foliation  $S_1$ , was affected by  $F_3$  folding. No penetrative planar structure is associated with  $F_3$  folds. Local development of fracture clearance ( $S_2$ ) in competent layers parallel to  $F_3$  axial plane is observed (Figure 11).  $S_1$  foliations swings around  $F_3$  closure (Figure 22). Broad swings in the trend of  $S_0$  are also noticed.  $F_3$  fold axes show variable plunge because of their super imposition on already folded surface.  $F_3$  minor folds are not common as  $F_1$  and  $F_2$  minor folds. However, several map scale  $F_3$  folds with constant orthogonal thickness and E-W to NW-SE axial trace are present. Variation in the trend of axial trace of the major fold can be attributed to superposed folds,  $F_3$  folding. Interference of  $F_3$  with  $F_1$  and  $F_2$  has resulted in doubly plunging folds.  $F_3$  major folds are identified at four places; 4 Km SSE of Kommandal, 8 Km SE of Bagmarpetai on the eastern limb of the Padagam  $F_2$  fold and 4 Km north of

Ganabapuram (Figure 2). In the eroded, dissected topography, these are expressed by broad synformal hills and narrow anti formal valleys. BMQ bands are often preserved in the closures of  $F_3$  major folds; the intervening portions having disappeared due to erosion.

3.4.4.  $F_4$  folds: are not expressed as minor folds. These are extremely broad regional flexures that have resulted in regional variations in the strike of litho units, especially in the southern and north western part of the area. (Figure 2).



Figure 11:  $S_2$  fracture cleavage developed parallel to the axial plane of  $F_3$  fold on  $S_0$  and  $S_1$  on BMQ

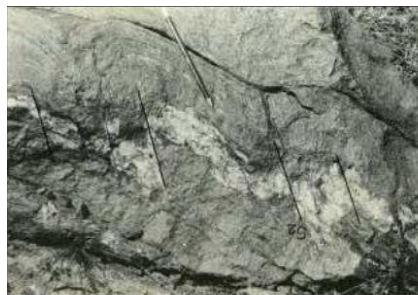


Figure 12: Shear fractures in BMQ



Figure 13: Geometry and orientation of folds of different phases



Figure 14: Eye shaped interference pattern in gneissic charnokite



Figure 15: Eye shaped interference pattern in pyroxene granulite



Figure 16: Nearly isoclinal  $S_1$  folds with thickened hinge and drawn out limb

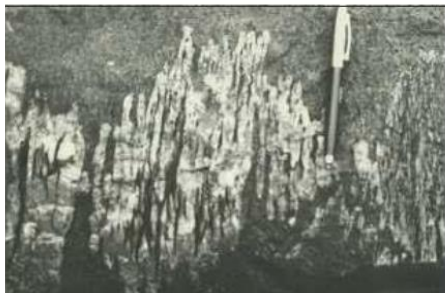


Figure 17: Extremely tight  $F_1$  fold in BMQ



Figure 18: Intrafolial  $F_1$  fold in BMQ



Figure 19: Rootless intrafolial fold in pyroxene granulite



Figure 20: Plunging  $F_2$  fold in BMQ



Figure 21: Co-axial minor  $F_1$  and  $F_2$  fold in BMQ

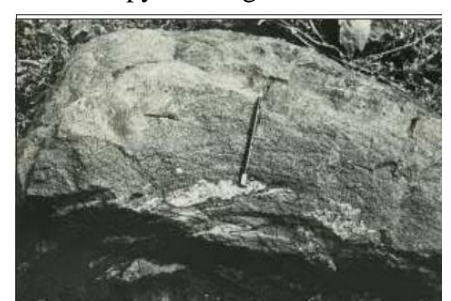


Figure 22:  $F_3$  fold in BMQ



Figure 23: Physiographically expressed F<sub>2</sub> Kommandal

### 3.5 Interference pattern

Due to the dominance of F<sub>1</sub> and F<sub>2</sub> folds, superposition of F<sub>1</sub> and F<sub>2</sub> folds are very common. Map scale interference is observed at Sananandal. Due to the effect of superimposition of F<sub>3</sub> on F<sub>1</sub>, and F<sub>2</sub>, F<sub>3</sub> folds warp the axial planes and hinges of F<sub>1</sub> and F<sub>2</sub> folds. Besides, eyed folds, due to the interference between F<sub>1</sub>, F<sub>2</sub> and F<sub>3</sub> have been noticed (Figure 15).

### 3.6 Faults

Faults observed in the area are shown in (Figure 2). The main criteria used for its recognition are; truncation of various lithological units, abrupt change in the attitude of beds, brecciated zones and cataclastic rocks. Faults have a consistent NW-SE trend and post-dates major folds. However, minor faults trending E-W, affect F<sub>3</sub> folds and predate F<sub>4</sub> deformation. F-F, the NW-SE trending fault is characterised by abrupt termination of BMQ ridge against charnockites and affect both BMQ and pyroxene granulite bands. The F'-F' fault is developed in the eastern limb of F<sub>4</sub> fold. The fault postdates F<sub>4</sub>. The NW-SE trending Fault affected both the limb of Sananandal and Nammiyandal folds.

### 3.7. Geometric analysis

It has proved to be the best method to analyse a large volume of data on spatial orientation of structural elements and draw meaningful conclusions. Construction of pie diagrams is the most satisfactory method for analyzing S-plane data in folded terrains. Lower hemispheric equal area projection is used for the geometric analysis of structural element. Foliation shows variation in attitude in different parts of the area.

### 3.8. Mechanism of formation of folds of different generations

The major F<sub>1</sub> Sananandal fold closure (Figure 1) and minor F<sub>1</sub> folds show considerable thickening of the hinge zone. In F<sub>2</sub> folds hinge thickening is not as pronounced as in F<sub>1</sub> folds. However some amount of thickening is observed in the Kommandal and Padagam F<sub>2</sub> folds (Figure 1). F<sub>3</sub> and F<sub>4</sub> folds are flexural folds as thickness is uniform in the limbs and the hinge. Thus there is a change in the mechanism of folding from Passive to flexural (Donath and Parker, 1964). This like the present area agrees well with the findings from other parts of the mobile belts. (Nair and Micheal, 1975; Nair 1977).

### 3.9. Mechanism of formation of fabric

Origin of tectonic fabric during deformation can be attributed to 3 main mechanisms- rotation of preexisting fabric (Williams 1976, 1977), Syntectonic recrystallization or crystalline including intragranular process (Spray, 1969) and intergranular process (White 1976, 1977). In most tectonites, at least two mechanisms might have been operative (Cosgrove, 1967; Mitra, 1976, 1978).

Most of the minerals are product of syntectonic crystallization during the F<sub>1</sub> phase of the DI event. During recrystallization, intra crystalline process, such as pressure solution (Rutter, 1983), might have played an important role in fabric development. Since most of the recrystallized grains are elongated parallel to foliation and show strain shadows, recovery and recrystallization probably took place during deformation (Dynamic recovery and Recrystallization). In the more strongly deformed rocks of the Kommandal closure (Figure 1) the quartz sub grains are smaller. This may possibly be related to high strains along the closure.

Durney (1976) suggested that dissolution would occur on grain faces, oriented at high angles to  $S_1$ , and accumulation would occur normal to  $S_1$  in the region of extension (Onasch, 1983; Wintsch, 1985). In the present study, grain elongation in the direction of foliation suggests that pressure solution also might have contributed to the flattening and elongation of grains. Undulos extinction, elongate grains and bent twin lamellae identified under microscope are effects of effects of intra crystalline deformation (George, 2014). Thus it can be concluded that during the  $D_1$  event recrystallization and intergranular processes were initiated along with intragranular process. These mechanisms were dominant during  $D_1$  event. While recrystallization was subdued during the  $D_2$  event.

#### 4. Summary and Conclusion

The complex structural pattern observed in the area is the result of overprinting and interference of structures generated during different deformation events. Imprints of both penetrative and non-penetrative secondary planar and linear structures and folds of different generations are present throughout the area. Relict intraformational or penecentemporaneous folds and folds on the limbs of isoclinal  $F_1$  folds ( $F_0$ ) are the earliest fold structures. Detailed study shows that the different structures are produced during two deformational episodes  $D_1$  and  $D_2$ . Formation of  $F_1$  folds and synchronous development of penetrative foliation  $S_1$ , axial planar to  $F_1$ , took places during the first deformation episode  $D_1$ .

Foliation  $S_1$ , which is essentially the product of metamorphism and deformation, is marked by preferred planar orientation of pyroene prisms and flakes of biotite in pyroxene granulites. In BMQ, recrystallisation and flattening of quartz and magnetite grains are mostly controlled by  $S_0$ , except in  $F_1$  fold hinges. In gneissic charnockite,  $S_1$  in parallel to compositional banding ( $S_0$ ). Both map scale and minor  $F_1$  folds are observed mostly in BMQ where  $S_0$  surface is preserved. Because of the tightness of  $F_1$  fold, except in hinges,  $S_0$  and  $S_2$  are effectively parallel. Formation of  $F_1$  and  $S_1$  marks the culmination of the first phase of  $D_1$ .

$F_2$  folds, co-axial with NNE-SSW trending  $F_1$ , folds, deforming earlier  $S_0$  and  $S_1$  were formed during the

second phase of  $D_1$ . Since both  $F_1$  and  $F_2$  are co-axial distinction between the two based on axial orientation is not possible. Many minor  $F_2$  folds are more open than  $F_1$  folds. However some are similar to  $F_1$  in geometry. Differences in the rheological properties of rocks can cause such geometrical differences (Chadwick et.al 1985). No planar fabric is associated with  $F_2$ . Broad similarity in geometry and co-axial nature of  $F_1$  and  $F_2$  strongly suggest that they were formed in succession during different phases of  $D_1$  with the stress field essentially remaining the same, as reported in the Kolar schist belt of Karnataka (Ghosh and Sengupta, 1985) and elsewhere (Jacobson, 1983).

The imprint of the second deformational event  $D_{11}$  is visible throughout the area as mesoscopic  $F_3$  folds of large wavelength.  $F_3$ , expressed both as minor and map-scale folds trend E-W to NW-SE. Fracture cleavage  $S_2$  is associated with these folds. Open geometry, high inter-limb angle ( $130^\circ$ ), E-W to NW-SE axial trend with easterly or westerly plunge distinguish  $F_3$  from  $F_1$ , and  $F_2$ . The broad swing observed in foliation trends (Fig.2) are related to  $F_4$  folding.  $D_{11}$  structures are represented by broad open flexures ( $F_4$ ) on mesoscopic scale.  $F_4$  fold are not expressed as minor folds. Extremely broad open geometry, NNW-NW to SSE-SE trending axial trace etc., distinguishes  $F_4$  from  $F_1$ ,  $F_2$  and  $F_3$ . All the major faults identified in the area postdate  $D_1$  and  $D_{11}$  and have a consistent NW-SE strike. The conclusions arrived at from structural map and geometric analysis by preparing pie diagrams were further verified by the author by carrying out dynamic analysis of quartz – C axis orientation (George, 2014)

#### Acknowledgement

The author expresses his deep sense of gratitude to Prof. PKR Nair, former head, Department of Geology, University of Kerala for his constant encouragement and suggestions throughout the course of work. The author also expresses his gratitude to Dr. Yadeta Chemdesa, Assistant Professor, ASTU for his valuable suggestions and Dr. Solomon Kassa, Head Department of Geology, ASTU for the encouragement. The author acknowledges the financial help received from Council of Scientific and Industrial Research (CSIR) New Delhi, India.

## Reference

- Anhaeusser, C.R; Mason, R., Viljoen, M.J. and Viljoen, R.P. (1969). A reappraisal of some aspects of Precambrian shield geology. *Bull. Geol. Soc. Am*; 80, 2175-2200.
- Beukes, N.J. (1973). Precambrian iron formations of South Africa. *Econ. Geol*; 68, 960-1004.
- Cosgrove, J.W. (1967). The formation of crenulation cleavage. *Jour. Geol.Soc.London*, 132,155-178.
- Chadwick, B., Ramakrishnan, M. and Viswantha, M.N. (1985). Babudan - a late Archaean intracratonic Volcano sedimentary basin, Karnataka, Southern India. *Jour. Geol. Soc. India*, 26, 802-821.
- Donath, F. A and Parker, R. B. (1964). Foldsand folding. *Bull. Geol. Soc. Am.*, 75, 45-62.
- Dorr. J.V.N. (1965) Nature and origin of the high grade hematite ores of Minas Gerais, Brazil. *Econ. Geol.*, 60, 1-46.
- Durney, S.A. (1983). A regional tectonic studyof the Archean ChithradurgaGreenstone belts of Karnataka based on Landsat interpretation. *Jour.Geol. Soc.India*, 24, 167-184.
- George, A.V. (2014) Micro structural analysis of quartz C-axis orientation from Polur area,Thiruvannamali District,, Tamilnadu,South India. *Indian Minerologist*, 38 (2), 39-45.
- Ghosh and Sengupta, S. (1985). Superposed folding and shearing in the western quartzite of Kolar gold field. *Indian Jour. Earth, Sci.*, 12, 1-8.
- Goodinough, K.M., Crowley C.G., Krabbendan and Paney S.F. (2013). *New U-Pb age constraints for the Laxford shear zones NW Scotland. Evidence for techno magmatic processes associated with the formation of a paleo protetrozoic*. NERC open Research Archives /Publisher. Elsewere.
- Grew, E.S. and Manton, W.I. (1986). A new correlation of sapphirine granulites, in the Indo-Antartic metamorphic terraine. Late Proterozoic dates from the Eastern Ghats. *Precamb, Res.*33, 123-137.
- Gulley, G.L. (1985). A Proterozoic granulite facies terrain on Rean Mountain, Western Blue ridge belt, North Carolina-Tennessees. *Bull. Ged. Soc. Amer.* 96, 1428-1439.
- Hansan, E.C, Hickman, N.H., Grant N.K. and Newton, R.C., (1985 a). Pan-African age of 'Peninsula Gneiss near Maduri, S. India (Abst.). *EDS (Trans. Amer. Geo-phys. Union)* 66, 419-420.
- Hansen, E.C., Newton, R.C. and Janardhan A.S. (1985 b). Geochemistry, Geobarometry and fluid inclusions of a continuous prograde amphibolite-facies gneiss to charnokite succession in Southern Karnataka. In: Kroner, G.N. Hansen and A.M. Goodwin (Eds.), *Archacan Geochemistry*. Springer-Verlag, New York, 161-181.
- Hotland, J.H. (1900). The charnockite series, a group of Archean hypersthene rocks in peninsular India. *Mem.Geol. Surv. India*, 28, 118-249.
- Jacobson, C.E. (1983). Structural Geology of the Pelona Schist and Vincent thrust, San Gabriel Mountains, California. *Bull. Geo. Soc. Am.* 94, 753-767.
- Jackson, D.R.; Santhosh, M. Matthey, D.P. and Harris, N.B.W, (1988). Stable Isotope studies on granutite from the high grade terrain of southern India. *Jour. Goel. Soc. India*, 31, 37-39.
- Joy Gopal Ghosh, Martin-J. dewit and Zartman, R.E. (2004). Age and tectonic evolution of Neoproterozoic ductile shear zones of the Southern Granulate Terraine of India, with implications for Gondwana Studies AGU.108 *Advanced Earth and Space Science. Journal of Tectories*.
- Krishnan, M.S., (1958). *Geology of India and Burna*. Higginbothams, Madrass, 555 p
- Kroner, A., Wycuib, Wangb S.Q., Wangb, C.Q., Namchinic. (1988). A single zircon ages from high-grade rocks of the Janping Complex, Liaoning province, NE China. *16 (5-6)*, 519-532.
- Li Gang Zhon, Ming-Guo Zhai, Jun sheng Lu, Lei zhao, Hao-Zheng wing, Jia-Lin Wu; Bolu Y1 Zou, Hou Xi angshan ria-Hong Cu., (2017). Proterozoic metamorphism of high-grade granulite facies rocks in the North China carton. *Precambrian research*, 303, 520-547.
- Mahadevan, T.M. (1976). Some aspects of the evolution of the Indian Precambrian shield (Abst.). *Jour. Gel. Soc. India*. 17,142.
- Nair, P. K. R., and Michea G.P. (1975). Syn-foliation reclined folds from Eastern Ghat belt rocks of Palghat district, Kerala State. *Curr. Sc.*, 44, 230.
- Nair. P.K.R. (1977). Age of Kalpete granite, Kerala State. *Curr. Sci.*, 44, 230.
- Onasch, C.M. (1983). Dynamic analysis of rough cleavage in the Martinsburg formation Maryland. *Jour. Struct. Geol.*, 5, 73-82
- Park, R.G., and Tarrey J. (1987). The Lewision Complex: a typical Pre cambrian high grade terrain. *Geol. Soc. London, spl. Public*, 27, 13-25.
- Raith, M., Raase, P., Ackerman, D, and Lal, R.K. (1983). Regional geothermometry in the granulite facies terrain of South India. *Trans. R. Soc. Edin Burgh. Earth Sci.*, 73, 221-244.

- Rutter, E.H. (1983). Pressure solution in nature, theory and experiment. *Jour. Geol. Soc. London*, 140, 725-740.
- Spray, A. (1969). *Metamorphic textures*. Pergamon Press, New York, 350p.
- Sugavanam, E.B., Venkata Rao, V., Simhachalam, J., Nagal, S.C. and Simha, A.K. (1976). Multiphase basic and ultrabasic activity in granulite terrane of North Arcot district, Tamilnadu. *Jour. Geol. Soc. India*, 17, 159-160.
- Swaminath, J. and 13 others. (1974). The cratonic greenstone belts of Southern Karnataka and their possible relation to the charnockite mobile belt. *Geol. Surv. India, Misc. Publ. No. 34*, 191-207.
- Talari Ramakrishnaiah Chetty and Baskara Rao, Y.J. (2006). The cauvery shear zone, Southern Granulite Terraine, India: A crustal scale Flevon structure. *Gondwana Research* 10(1-2) 77-85.
- White, S.H. (1976). The effects of strain on microstructures, fabric and deformation mechanisms in quartzites. *Phil. Trans. R. Soc. London*, 283, 69-86
- Wintsch, R.P. (1985). *The possible effects of deformation on chemical process in metamorphic fault zones*. In: A.B. Thompson and D.C. Ruble (Eds.). *Metamorphic reactions*, Springer-Verlag, New York, 251-268.
- Williams, P.F. (1976). Relations between axial plane foliations and strain. *Tectonophysics*, 30, 181-196.
- Williams, P. F. (1977). Foliation a review and discussion. *Tectonophysics*, 10, 181-196.